PUT YOUR MASCON: IMPLEMENTING THE MASCON-LAYER MODEL INTO THE N-BODY INTEGRATOR *REBOUND*

J. N. Larson[1], F. C. F. Venditti[2], G. Sarid[3], and Y. R. Fernandez[1], [1]University of Central Florida (4000 Central Florida Blvd, Orlando, FL, 32816; jlarson27@Knights.ucf.edu), [2]Arecibo Observatory – University of Central Florida (PR-625, Arecibo, 00612, Puerto Rico), [3]SETI Institute (189 Bernardo Ave #200, Mountain View, CA 94043).

Introduction: Detailed maps of potential fields around asteroids and other small bodies allow us to better understand how to navigate and land spacecraft, collect samples, trace debris evolution over time, and more. Previous gravity field models include the Werner method [1,2] which involves dividing the body's surface into facets that represent a portion of the body's mass. From these mascons, the gravitational potential across the surface is calculated and gravitational influence can be found at a given point by summing the potential of each facet experienced at the given point. While this method is accurate, it is also very computationally intensive and has room for error, namely, it fails to account for varying material densities within the body.

In our initial development of the *Rebound* Ejecta Dynamics (RED) package [3,4] to account for non-spherical gravity fields that are common among small asteroids, we implemented an ellipsoidal gravitational potential. While this method is a better approximation of larger, less irregular asteroids, it is still merely an approximation and does not apply to objects that are not ellipsoids.

The Venditti method [5,6] examined here starts with the 3-D shape of an asteroid as derived from Arecibo Observatory and Goldstone radar data and divides the body into mascons within the body rather than simply surface facets. With this method we sum the gravitational potential from each mascon to calculate the total potential at a given point. This method is less computationally intensive depending on the resolution chosen when forming mascons and allows for varying material properties within the body itself since the interior of the body, not just the surface, is being divided into mascons.

Here we introduce the Venditti method into the Python N-body integrator *Rebound* [7] as an independent function. We bench-mark this function against the RED package simulations of the Double Asteroid Redirection Test (DART) impact set to occur in fall 2022 [8]. Extensive data of the system's gravitational potential will continue to be collected after the impact, providing us with experimental data both at the surface and system wide scale to which our model can be compared.

Methodology: Radar data from Arecibo and Goldstone Observatories let us derive the shape of an asteroid with a series of points. By connecting neighboring points, we cover the surface in facets that represent a quantity of mass that makes up the asteroid. The facet vertices are extended down to the barycenter of the body and divided into layers as shown in fig. 1. (from [6]). The surface of the asteroid is on the right, and there are five mascons delineated down to the center at left.

To add an irregularly shaped object into a *Rebound* simulation, the object's gravitational potential must be input as a force acting upon a particle in space. At each time step a new force will be calculated corresponding to that particle's new position relative to the surface. Since so many calculations can bog down the simulation rather quickly, it is crucial to use the smallest number of mascons without sacrificing the precision of the calculation. Here we use five layers as was shown to be sufficient by [6].

In anticipation of the DART mission, we benchmark our code against Dimorphos and Didymos. While the exact shape of Dimorphos is still unknown, the shape of Didymos has been constrained [9] from radar data, allowing us to test the implementation of the mascon-layer model into RED using Didymos (without the secondary in the system) as a test body. We first set up a spherical representation of Didymos with a radius of 400m and a mass of 5.23×10^{11}kg in a *Rebound* simulation. Our second test scenario uses the RED ellipsoidal gravity approximation with an ellipsoidal Didymos with axes a=420m, b=390m, and c=365m. Finally, we implement the mascon-layer model described above to calculate a gravitational potential that varies based on surface terrain and variations in density throughout the body. A test particle is set into orbit 150m above the equator in each simulation.

Results: First, we examine the baseline scenario of a test particle orbiting a spherical Didymos. As expected, the particle maintains a stable circular orbit about the equator without changes in eccentricity or inclination. Figure 2a shows an xy-projection of this circular orbit in orange. We also examine the ellipsoidal case using the ellipsoidal gravity calculated by the RED function. Since Didymos is a rather spherical body, we do not see any significant differences between the spherical case and the ellipsoidal case. We will test the ellipsoidal scenario compared to the mascon-layer method on more elongated bodies such as Kleopatra in future benchmark studies.

Finally, we examine the orbit of a test particle around the radar derived shape of Didymos. While the orbit here has the same initial conditions as in the spherical and ellipsoidal approximation cases, the orbit for this case (shown in blue in fig. 2a) becomes unstable over time. We notice the orbit becomes less centered around the origin and the eccentricity increases due to variations in the surface topology. Figures 2b,c,d respectively show the differences between the mascon-layer model and the spherical model for the distance of the particle from the center of the body, the eccentricity of the orbit, and the inclination of the particle relative to the equatorial plane. We notice that in the radar derived scenario, the particle's orbit oscillates so that the center of the orbit is no longer the same as the center of the circular orbit; however, the eccentricity does not change significantly. While this orbit remains fairly circular it wobbles about where the orbit falls in the spherical case.

Discussion and Future Work: These differences in orbits, even with a relatively spherical asteroid, point out the importance of implementing a shape model over a spherical or ellipsoidal approximation of a small body. Small deviations in surface topology can have significant effects on particles near the surface, such as during impact events.

To further explore the advantages of using the mascon-layer model in RED, we must examine a large selection of very diverse asteroid shapes. Due to recent missions to asteroids, we have better characterized the gravity fields around these objects, setting them up to be prime benchmarks for this new component of RED.

Acknowledgments: The authors thank the Center for Lunar and Asteroid Surface Science (CLASS) for their continued support of this project.

References: [1] Werner, R. A. (1994) *CeMDA, 59,* 253-278. [2] Werner, R. A. and Scheeres, D. J. (1996) *CeMDA, 59,* 313-344. [3] Larson, J. N. et al. (2020) *LPS LI,* Abstract #2133. [4] Larson, J. N. and Sarid, G. (2021) *MNRAS*, in press. [5] Venditti, F. C. F. et al. (2013) *J. Phys. Conf. Ser., 465,* 012008. [6] Venditti, F. C. F. and Rocco, E. M. (2018) *Advances in the Astronautical Sciences Series, 162,* 2041-2060. [7] Rein, H. and Liu, S. F. (2012) *A&A, 537,* A128. [8] Cheng, A. et al. (2018) *P&SS, 157,* 104-115. [9] Naidu, S. P. et al. (2020) *Icarus, 348,* 113777.

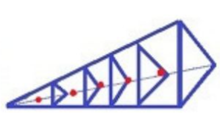

Figure 1. An example from [6] of how each facet on the surface (at right) is extended to the center of the body (at left) and separated into layers (in this case, five). The mascons are then assigned to points (red dots) in the center of each layer.

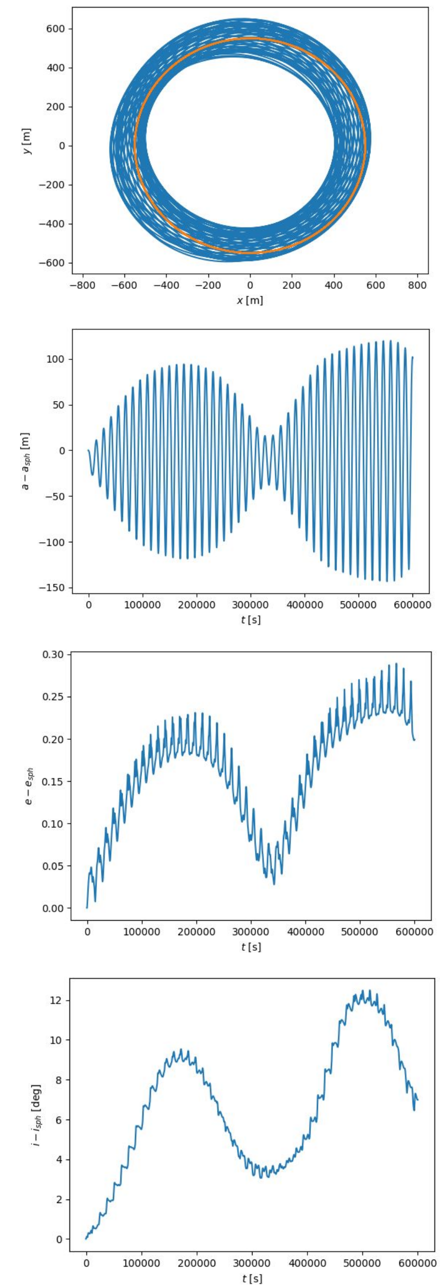

Figure 2. (a) An xy-projection of the orbit about a spherical body (orange) and the orbit about the body built with the mascon-layer model (blue). (b) The distance from the mascon-layer test particle to the center of the body minus the spherical case test particle to the center of the body. (c) The eccentricity of the mascon-layer test orbit minus the spherical test orbit.. (d) The inclination (in degrees) of the mascon-layer test orbit minus the inclination of the spherical test orbit.